Published in Optics Letters 24, issue 2, 71-73, 1999
which should be used for any reference to this work

Diffraction from metallic gratings with locally varying profile forms

Wayne R. Tompkin and René Staub
OVD Kinegram Corporation, Advanced Research, CH-6301 Zug, Switzerland

Andreas Schilling and Hans-Peter Herzig
Institute of Microtechnology, University of Neuchâtel, CH-2000 Neuchâtel, Switzerland

Measurements of the diffraction characteristics of one-dimensional surface-relief gratings of locally varying profile are compared with rigorous diffraction theory. These gratings result from the superposition of two linear sinusoidal gratings of uniform depth for which the relative phase between the two gratings varies slowly with position. The resultant surface profile exhibits a relatively large-period variation in profile form. The periodic variation in diffraction efficiency that results yields a visual moiré pattern that has interesting asymmetry and polarization properties that alter as the viewing conditions are changed; the gratings can be exploited by diffractive optically variable devices for document security.

Superposing two or more diffractive surface-relief structures can produce a surprisingly rich family of diffractive structures.[1] Indeed, through the seemingly straightforward superposition of sinusoidal holographic gratings, any continuous profile form can theoretically be synthesized.[2] Technical constraints effectively limit the range of diffractive structures that can be realized in practice; however, the experimental difficulties of superimposing two exposures for a grating of reasonable extent have been overcome to produce blazed gratings through Fourier synthesis.[3]

In contrast to realizing large-area homogeneous Fourier gratings, which has been the goal of previous research, we have combined two sinusoidal gratings for which the relative phase between the two superposed sinusoids is allowed to vary, resulting in a profile that varies with position. An advantage of gratings of locally varying profile form is that they are useful for the study of the diffraction properties of a class of profiles. Indeed, while the profile form varies continuously, one can obtain information that might be missed when a set of discrete samples is produced and studied. Furthermore, surface-relief gratings of locally varying profile can display visual effects, such as bands of color that change in contrast and hue as the grating is tilted. As these visual effects can be clearly differentiable from those of standard holographic gratings, surface-relief gratings of locally varying profile are potential visual security elements. Such visual security devices based on diffraction phenomena are known as optically variable devices.[4]

We have realized samples in which the relative phase between the two sinusoids is a function of position by using at least one basis function with a slowly varying period. In particular, we have combined a 2000-line/mm sinusoidal grating with a 1000-line/mm sinusoidal grating, where the phase β between the fundamental and the first harmonic is a slow function of position. The two surface-relief profiles that we combined can be described by the functions $f_1(x)$ and $f_2(x)$:

$$f_1(x) = b_1 \sin[2Kx + \beta(x)], f_2(x) = b_2 \sin(Kx), \quad (1)$$

where the subscripts 1 and 2 refer to the order in which the gratings are written in our experiments, the magnitude of the grating vector of the fundamental K is $2\pi/d_2$, and the period of the fundamental d_2 is approximately 1 μm. The grating amplitudes b_1 and b_2 were approximately equal to the first two Fourier coefficients for a triangular grating, $2b_1 = b_2$. The resultant surface-relief profile is described by $f_3(x, y) = f_3(x) = f_1(x) + f_2(x)$, where the grooves of the two sinusoidal basis gratings are parallel.

The combination sinusoidal grating was realized through the double exposure of a photoresist plate. In the first exposure the higher-frequency grating was written through the interference of two spherical waves emanating from two pinholes, P_1 and P_1', which were separated by a distance $2x_1 = 0.92$ m at a distance $z_1 = 1.00$ m from the photoresist plate (Fig. 1). The grating was exposed by use of a single-frequency krypton-ion laser operating at $\lambda = 413.1$ nm. The surface profile of the photoresist following exposure was approximately

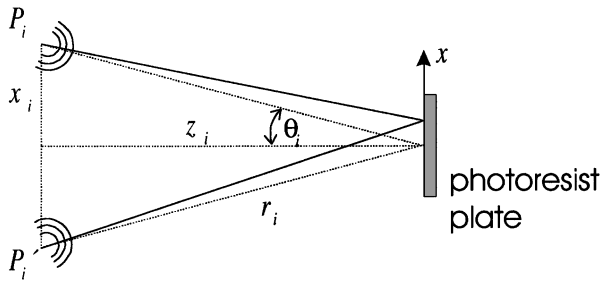

Fig. 1. Schematic of the experimental setup used to write the gratings. Spherical waves emanate from two pinholes, P_i and P_i', which are separated by a distance $2x_i$. These waves interfere at the photoresist plate a distance z_i from the line connecting the two points.

proportional to the intensity pattern $I_1(x)$ of the exposing light. The grating had a spatial frequency $d_1{}^{-1}(x)$ that decreased approximately quadratically with respect to distance x, which is perpendicular to the groove direction, as shown in the formula for the spatial frequency as derived from the expression for the interference pattern of the exposure:

$$I_i(x) = 4I_i(0)\cos^2\left[\frac{\pi}{\lambda}\,\mathrm{OPD}_i(x)\right],$$

$$\mathrm{OPD}_i(x) \approx 2x\,\sin\theta_i\left[1 - \frac{1}{2}\cos^2\theta_i\left(\frac{x}{r_i}\right)^2\right],$$

$$d_i{}^{-1}(x) = \frac{1}{\lambda}\,\frac{\partial \mathrm{OPD}_i}{\partial \chi} \approx \frac{2\sin\theta_i}{\lambda} \times \left[1 - \frac{3}{2}\cos^2\theta_i\left(\frac{x}{r_i}\right)^2\frac{\partial \mathrm{OPD}_i}{\partial \chi}\right], \qquad (2)$$

where the subscript i is 1 and 2 for the first and second exposures, respectively, $I_i(0)$ is the intensity of each beam at the photoresist plate, OPD_i is the optical path difference, $r_i{}^2 = x_i{}^2 + z_i{}^2$, $\sin\theta_i = x_i/r_i$, and $x \ll r_i$.

For the second exposure, the pinholes were moved closer together ($2x_2 = 0.42$ m) such that the spatial frequency of the first exposure would be twice that of the second exposure at a point on the photoresist plate. We translated the photoresist plate by a distance $\Delta = -25$ mm along x and 2.5 mm toward the pinhole to fine tune the spatial frequency of the second exposure. The exposure time of the second exposure was twice that of the first exposure when the intensity was held constant. The photoresist plate was developed, and nickel shims were fabricated from the photoresist plate through electroforming.

The surface profile of the final combination grating was determined with an atomic-force microscope (AFM). Typical surface profiles of the nickel shim for four distinct values of the relative phase are shown in Fig. 2. The period of the combination grating was determined from the AFM measurements to be 1015 ± 15 lines/mm, and we found the amplitude of the fundamental b_2 to be approximately 70 nm by fitting the measured profiles to Eqs. (1) for various values of β. From Fig. 2 one sees that for $\beta = 0°$ ($x = 0$ mm) there is a blaze pointing right and for $\beta = 180°$ ($x = 1.25$ mm) there is a blaze pointing left. Furthermore, there is a dip at the top for $\beta = 90°$ ($x = 0.85$ mm) and a bump on the bottom for $\beta = 270°$ ($x = 4.7$ mm).

As can be seen from Eqs. (2), the line densities of both gratings f_1 and f_2 have quadratic dependencies on position. In the sample studied, the period of the second grating f_2 was fairly constant over the area of measurement; thus Eqs. (1) describe the combination grating. From AFM measurements, the functional form of the slow variation of β can be determined and is shown in Fig. 3; the relative phase shift β varied from 0° to 180° over 1.25 mm.

A scalar description of grating diffraction might be appropriate to give a qualitative understanding of the phenomenon, yet scalar theory gives reliable results only when the ratio of the period to the wavelength (d/λ) is greater than approximately 5–10. For a quantitative understanding of the experimental results for the combination gratings, for which this ratio was ~1.7, exact electromagnetic theory must be applied. For the grating diffraction calculations we used a rigorous eigenmode method as described by Turunen,[5] whereas the solution of the boundary equations is handled following the method of Moharam and Gaylord.[6] We modified the implementation according to Moharam *et al.*[7] to avoid numerical instabilities that originated from the successive matchings of the electromagnetic boundary conditions at the interfaces. Additionally, the implementation was improved according to the formulation of Lalanne and Morris.[8] These modifications are especially advantageous for calculating highly conductive metallic gratings in TM polarization to ensure a well-defined convergence of the solutions. All calculations were done for a linearly polarized plane wave incident normally from air. We carefully checked the convergence of all solutions.

We measured the diffractive characteristics as a function of profile form by illuminating an area that

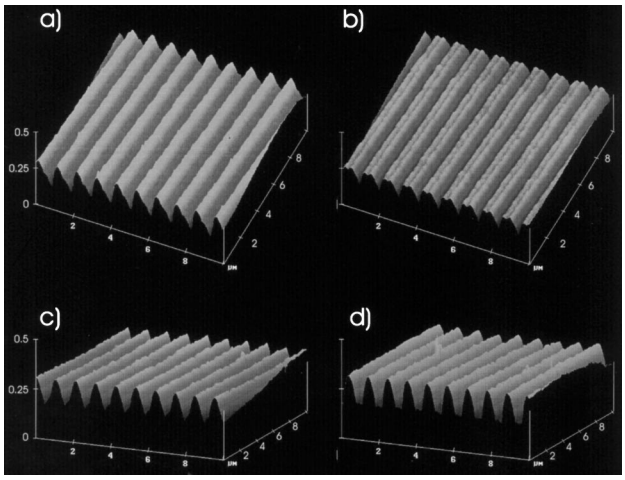

Fig. 2. Typical surface-relief measured profiles for values of β of (a) 0°, (b) 90°, (c) 180°, and (d) 270°. The peak-to-peak profile heights of the measured profiles are (a) 145, (b) 115, (c) 140, and (d) 170 nm.

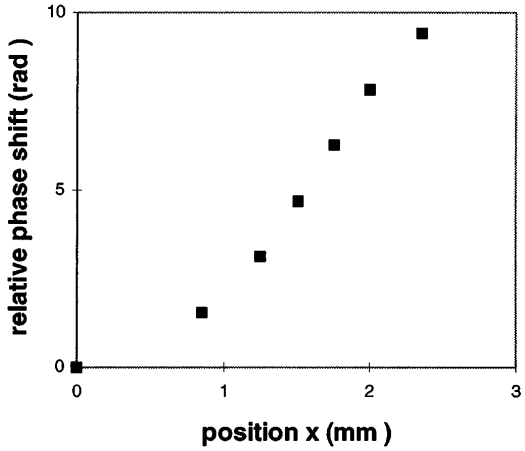

Fig. 3. Relative phase shift between the two basis functions versus position x, as determined from AFM measurements.

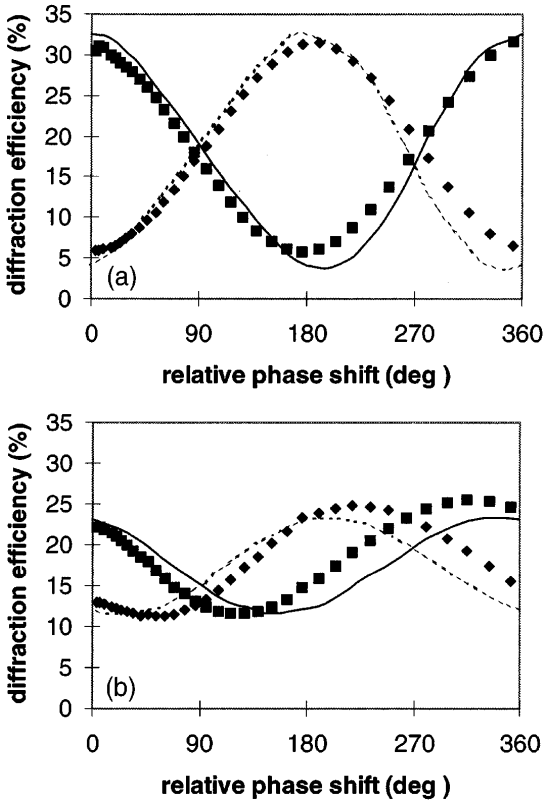

Fig. 4. Measured and calculated diffraction efficiency (in percent) as a function of the relative phase β in degrees for the $+1$ and -1 orders for (a) TM and (b) TE illumination. The measured diffraction efficiencies are shown as filled squares for the $+1$ order and as filled diamonds for the -1 order; the calculated values are shown as solid and dashed curves for the $+1$ and -1 orders, respectively.

had dimensions much smaller than the distance over which the relative phase changes significantly. A focused He–Ne laser with a wavelength of 632.8 nm illuminated the combination gratings at normal incidence through air; the spot size was 30 μm at the surface. Whereas well over ten grating periods are illuminated, the measured values for the diffraction efficiencies should be essentially equivalent to the case in which an infinite number of periods is illuminated.[9] In Fig. 4 we plot the intensity of the $+1$ and -1 orders for TE as well as for TM polarizations as a function of the relative phase β. Several phenomena can be seen from the curves: First, we see that the $+1$ order is much more intense than the -1 order when the blaze points to the left ($\beta = 0°$) and is much less than the -1 order when the blaze points to the right ($\beta = 180°$). Second, we see that for the points where the profile form is symmetric, $\beta = 90°$ and $\beta = 270°$, the $+1$ and -1 orders are equal, as expected, for TM polarization; however, for TE polarization the profile form where the high-frequency modulation is deep in the profile ($\beta = 270°$) has a different value for diffraction efficiency than is the case when the modulation is on the surface of the profile ($\beta = 90°$). Furthermore, the sample was interesting visually: The resultant moiré fringes changed in contrast as the sample was tilted as well as when the polarization of the illumination was altered or a polarizer was rotated in front of the eye.

Figure 4 displays the results of measured and rigorously calculated diffraction efficiencies for nickel combination gratings with a relative phase shift of 0°–360°. For the calculation we used $b_2 = 2b_1 = 70$ nm, and the refractive index of nickel for a wavelength of 632.8 nm was $n = 1.8 + 3.3i$, as determined by ellipsometric measurements. The agreement between calculated and measured values is quite satisfactory. The small deviations between the experimental and theoretical values for the diffraction efficiencies can be explained by slight absolute height variations of the grating structure. In comparing the scalar results[3,10] with the exact values obtained by rigorous diffraction theory as in Fig. 4, one can see that scalar theory predicts the correct qualitative behavior, whereas the absolute values can differ considerably from the values for TE and TM polarization.

In conclusion, we have realized one-dimensional surface-relief gratings of locally varying profile through the superposition of two linear sinusoidal gratings of uniform depth for which the relative phase between the two gratings varies slowly with position. The resultant surface profile exhibited a relatively large-period variation in profile form and, thus, in diffraction efficiency. The measured values for the diffraction characteristics showed good agreement with the values of rigorous diffraction theory. The sinusoidal superpositions of locally varying phase displayed a moiré pattern that altered as the viewing conditions were changed, a property that can be exploited for optically variable devices.

The authors acknowledge the collaboration of J. S. Pederson and M. T. Gale of the Centre Suisse d'Electronique et Microtechnique, Zurich. This project was supported in part by the Swiss priority program Optique II, Micro-Optics.

References

1. R. Staub, W. R. Tompkin, and J.-F. Moser, Proc. SPIE **2689,** 292 (1996).
2. E. G. Loewen and E. Popov, *Diffraction Gratings and Applications* (Marcel Dekker, New York, 1997), pp. 531–554.
3. S. Johansson and K. Biedermann, Proc. SPIE **240,** 44 (1980).
4. J.-F. Moser, in *Optical Document Security*, R. van Renesse, ed. (Artech House, London, 1998), pp. 247–266.
5. J. Turunen, in *Micro-Optics, Elements, Systems and Applications*, H.-P. Herzig, ed. (Taylor & Francis, London, 1997), pp. 31–52.
6. M. G. Moharam and T. K. Gaylord, J. Opt. Soc. Am. **72,** 1385 (1982).
7. M. G. Moharam, D. A. Pommet, E. B. Grann, and T. K. Gaylord, J. Opt. Soc. Am. A **12,** 1077 (1995).
8. P. Lalanne and G. M. Morris, J. Opt. Soc. Am. A **13,** 779 (1996).
9. K. Hirayama, E. N. Glytsis, and T. K. Gaylord, J. Opt. Soc. Am. A **14,** 907 (1997).
10. W. R. Tompkin and R. Staub, Proc. SPIE **3291,** 1 (1998).